

Ring Formation Drives Invagination of the Vulva in *Caenorhabditis elegans*: Ras, Cell Fusion, and Cell Migration Determine Structural Fates

Gidi Shemer, Ranjana Kishore,¹ and Benjamin Podbilewicz²

Department of Biology, Technion–Israel Institute of Technology, Haifa, 32000, Israel

Directed cell rearrangements occur during gastrulation, neurulation, and organ formation. Despite the identification of developmental processes in which invagination is a critical component of pattern formation, little is known regarding the underlying cellular and molecular details. *Caenorhabditis elegans* vulval epithelial cells undergo morphological changes that generate an invagination through the formation of seven stacked rings. Here, we study the dynamics of ring formation during multivulva morphogenesis of a *let-60/ras* gain-of-function mutant as a model system to explore the cellular mechanisms that drive invagination. The behavior of individual cells was analyzed in a *let-60/ras* mutant by three-dimensional confocal microscopy. We showed that stereotyped cell fusion events occur within the rings that form functional and nonfunctional vulvae in a *let-60/ras* mutant. Expression of *let-60/ras* gain-of-function results in abnormal cell migration, ectopic cell fusion, and structural fate transformation. Within each developing vulva the anterior and posterior halves develop autonomously. Contrary to prevailing hypotheses which proposed three cell fates (1°, 2°, and 3°), we found that each of the seven rings is a product of a discrete structural pathway that is derived from arrays of seven distinct cell fates (A, B, C, D, E, F, and H). We have also shown how autonomous ring formation is the morphogenetic force that drives invagination of the vulva. © 2000 Academic Press

Key Words: organogenesis; vulva development; *Caenorhabditis elegans*; cell fusion; cell migration; *let-60*; Ras; invagination; morphogenesis; epithelia.

INTRODUCTION

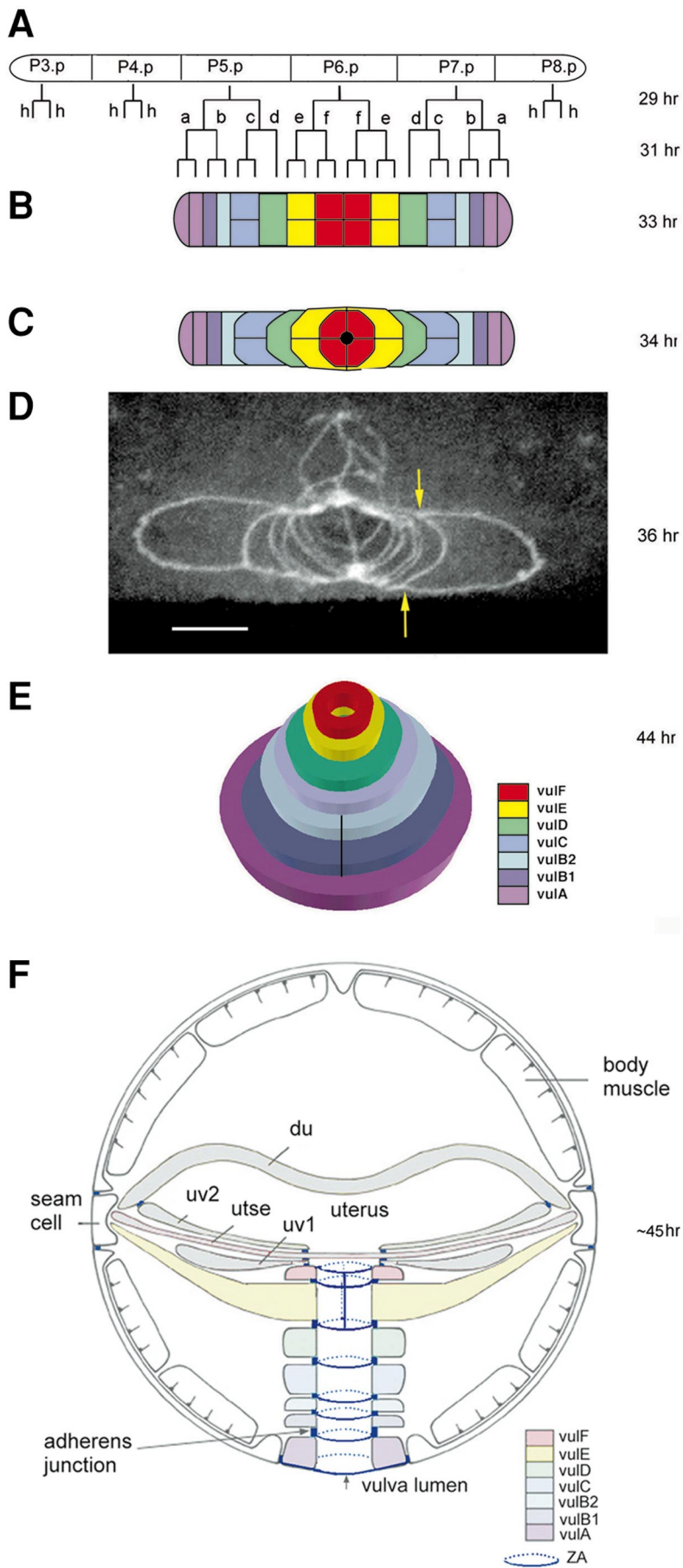
Organogenesis is the process of laying down the basic body plan in an organism. During organogenesis various cellular events such as cell migration, cell–matrix interaction, cell–cell interaction, and cell fusion act in concert for the production of specific organs and structures. One of the best models for studying organogenesis is the vulva of the nematode *Caenorhabditis elegans*. This organ is formed from only 22 epithelial cells yet its formation involves all the major features of organ development. The vulva has been studied extensively and much is known about the signaling pathways and the genetic interactions during the early phases of vulval development (Greenwald, 1997). However, only recently the cellular events that take place

during the later stages of vulva formation have been described (Sharma-Kishore *et al.*, 1999).

During the first larval stage (L1) six vulval precursor cells (VPCs), all of them having the potential to participate in vulva formation, are generated from ventral hypodermal cells (Sulston and Horvitz, 1977; Kimble, 1981). These cells (P(3–8).p) are subjected to at least four signaling pathways: an RTK-RAS-MAP kinase pathway induced by the gonadal somatic anchor cell (AC) that along with a Wnt pathway affect P(5–7).p to adopt vulval cell fates (Han *et al.*, 1990; Lackner *et al.*, 1994; Wu and Han, 1994; Eisenmann *et al.*, 1998; Maloof and Kenyon, 1998), a LIN-12/NOTCH lateral signaling pathway that determines the 1° sublineage of P6.p and the 2° sublineages of P5.p and P7.p (Greenwald *et al.*, 1983), and a LIN-15 inhibitory signaling pathway that induces P3.p, P4.p, and P8.p to generate a 3° sublineage, that is, fusion to the surrounding hypodermal syncytium hyp7 (Herman and Hedgecock, 1990; Thomas and Horvitz, 1999). The consequence of all these signals is the formation of a twofold symmetrical primordium of 22 cells. The organo-

¹ Current address: Department of Genetics, University of Pennsylvania School of Medicine, Philadelphia, PA 19104.

² To whom correspondence should be addressed at Department of Biology, Technion-ILT, Haifa, 32000, Israel. Fax: (972) 4 822 51 53. E-mail: podbilew@tx.technion.ac.il.



1

genesis of the vulva is summarized in Fig. 1. This process begins as cells from each half of the primordium undergo short-range migrations toward the primordium's midline until meeting with their symmetrical partners from the other half, thus pushing the inner cells dorsally and creating an invaginated stack of seven toroids. This is followed by cell fusion within five of these toroids and attachments of specific toroids to specific epithelial cells and vulval muscle cells. During this time the AC invades the most dorsal ring and then fuses to the utse cell. The last stage involves eversion of the vulva forming a functional tube-shaped organ (Sharma-Kishore *et al.*, 1999).

One of the central players in the inductive machinery is the LET-60/RAS protein, which acts as a switch in the determination between vulval and nonvulval fates (Beitel *et al.*, 1990; Han *et al.*, 1990). Loss-of-function (*lf*) mutations in the *let-60* gene give rise to a vulvaless (Vul) phenotype as a result of the 3° sublineage adopted by all the VPCs. Gain-of-function (*gf*) mutations involve the adoption of 1°/2°/3° sublineages by VPCs that normally adopt only the 3° sublineage and result in a multivulva (Muv) phenotype, in which additional vulva-like structures are generated independently of the presence of the AC (Ferguson *et al.*, 1987; Beitel *et al.*, 1990). RAS, as well as other small GTPases like the Rho family proteins, takes part not only in general proliferation but also in developmental events such as cell migration (reviewed in Sternberg and Han, 1998).

In this study we have analyzed a *let-60/ras(gf)* mutant in order to define the minimal requirements for each and every cellular event during vulva formation. To understand the mutual relationships between the real (functional) and pseudo (additional and nonfunctional) vulvae

characteristic to this Muv mutant, we have asked four questions:

1. How does a pseudovulva develop and how does this differ from normal vulva development?
2. Do vulval cells migrate autonomously or attract each other, or is there an external signal that induces migration?
3. Do vulval cells fuse only with homologous cells (e.g., A with A)?
4. Does Ras signaling influence cell fusion and cell migration during vulva formation?

First, we have described the complete cellular events taking place during the generation of a Muv mutant. Second, we found out that within each primordium, each half develops autonomously throughout the entire vulvae organogenesis. As the different primordia develop, they compete with each other for vulval cells, resulting in the formation of asymmetrical vulvae. Third, we have observed that the ultimate fate of the VPC's descendants is to produce a structural scaffold which lines the vulval opening and that cells can attain differentiated structural states of absent cells to complete the minimal requirements for vulva formation. Finally, we provide evidence suggesting that RAS may influence the migration and fusion fates of certain cells during vulva formation.

MATERIALS AND METHODS

General Methods and Strains

Methods for the culturing and handling of worms were as described before (Brenner, 1974). Animals were raised at 20°C unless otherwise stated. *C. elegans* strain N2 was the wild-type

FIG. 1. Vulva formation in the wild type (A). **FIG. 1.** The vulva precursor cells (VPCs; P(3-8).p) execute their cellular fate in the mid-L3 stage depending on their signaling. P3.p, P4.p, and P8.p divide once and fuse to the surrounding hypodermal syncytium *hyp7*. (B) P(5-7).p undergo three rounds of divisions yielding a primordium of 22 cells. Six cell fates established in a palindromic sequence (a-f f-a) are the precursors of the structural differentiated states (vulA-vulF). h, cells fused to *hyp7*. (C) At the onset of the L4 stage, the cells send unidirectional processes ventrally and laterally toward the midline of the primordium creating an invagination. These short-range migrations take place in a spatial and temporal order starting with the e cells and ending with the external a cells resulting in a stack of seven toroids or rings. Black dot represents the anchor cell (AC). (D) Confocal micrograph of a vulva primordium stained with MH27 mAb that reveals apical domains, adherens junctions, or zonula adherens (ZA) of cells (Sharma-Kishore *et al.*, 1999). In each half of the primordium the precursors of vulA fused before they started their migrations and the precursors of vulC have fused after they completed their migrations. The yellow arrows point to two filopodia derived from the posterior binucleate a cell. This intermediate is before intratoroidal cell fusion and the central vulF and vulE rings on the top are already more dorsal than the external rings. (E) The cells within the rings (except for vulB1 and vulB2) fuse in a temporal order and the gonadal AC fuses to the uterine utse cell resulting in the formation of a tube-shaped L4 vulva. (F) Transverse section of the body of a late L4 stage showing the connections between the vulva and the cells of the uterus (uv1, utse, uv2, and du) and between the vulva and the hypodermis (*hyp7* in the ventral side and seam cells on the left and right). The lumen of the vulva shows cylindrical zonula adherens (ZA, in blue; dotted line is posterior) that link the apical domains of the different cells. VulA ring connects to the hypodermis in the ventral side, vulF connects to the uv1 cell of the uterus on the dorsal side, and the apical domains of all the adjacent rings are linked to each other (e.g., vulA to vulB1 and vulF to vulE). The transverse junctions between the cells of the vulF and vulE rings are shown here as vertical lines before they fuse. The same color code for the different cell types and the vulval rings has been maintained for all the figures except for (F). Anterior is to the left except for (F) that is a transverse section in which dorsal is to the top. (B, C) Dorsal views. Nomenclature: a-h are the cell fates of the VPC granddaughters. The use of lowercase here and in Figs. 2 and 3 is simply to differentiate the cell fates from the uppercase letters of the panels (see also Fig. 5). The cellular sublineages and the times in hours after hatching at 20°C are from Sulston and Horvitz (1977). The figure is modified from Sharma-Kishore *et al.* (1999).

strain (Brenner, 1974). The following strains were used: LGIV: *let-60(n1046)* (Beitel *et al.*, 1990; Han and Sternberg, 1990). BP74 *let-60(n1046) jclS1[MH27-GFP]* was obtained by mating males expressing MH27-GFP (Mohler *et al.*, 1998) with *let-60(n1046)* hermaphrodites and selecting recombinant progeny that expressed the Muv phenotype as well as fluorescent apical junctions of epithelial cells. The *jclS1* strain (kindly provided by J. Simske and J. Hardin (Mohler *et al.*, 1998)) contains all known control sequences required to target MH27 to the cellular junctions, pRF4 (a plasmid containing the dominant roller mutation *rol-6(su1006)*) and F35D3 (*unc29+* DNA) in an N2 background (*unc-29* DNA was used to add complexity to the array). The presence of the dominant cuticle mutation *rol-6* in the *jclS1* strain is unlikely to affect morphogenesis since MH27 antibody was also used in *let-60(n1046)* without *jclS1*.

Permeabilization, Fixation, and Immunofluorescence

Worms were fixed and permeabilized as described before (Finney and Ruvkun, 1990; Sharma-Kishore *et al.*, 1999). Stages of development were determined by using Nomarski optics or by following the development of the seam cells through fluorescence microscopy (Podbilewicz and White, 1994). Immunofluorescence was carried out as described before (Podbilewicz, 1996; Sharma-Kishore *et al.*, 1999). The mouse monoclonal antibody MH27 (1:300 dilution) was used to stain the adherens junctions of epithelial cells (Francis and Waterston, 1991; Podbilewicz, 1996).

Confocal and Fluorescence Microscopy

Confocal reconstructions were made by using an MRC-1024, laser confocal scanning microscope (Bio-Rad, Hempstead, UK) with the objective Nikon Plan Apo 60 \times /1.40 (Podbilewicz, 1996; Sharma-Kishore *et al.*, 1999). Cell identity was revealed using the characteristic staining of the apical junctions of vulE and vulF (narrow and tall shape in the dorsoventral axis in 100 and ~65% of the vulvae, respectively; see Figs. 1 and 7) and vulB1-vulB2 (short rings compared with the rest) (Sharma-Kishore *et al.*, 1999). Worms were either anesthetized in 0.01% tetramisole, 0.1% tricaine, or paralyzed transiently by lowering the temperature to 8–11°C for 10–20 min using a temperature control system (Y. Rabin and B. Podbilewicz, unpublished results). Cell lineages were followed as described (Sulston and Horvitz, 1977).

RESULTS

Cellular Events during Vulva Formation

Organogenesis of the *C. elegans* vulva in wild-type animals can be divided into three phases (Fig. 1): short-range migration forming seven stacked rings, cell fusion, and eversion of the vulva (Sharma-Kishore *et al.*, 1999).

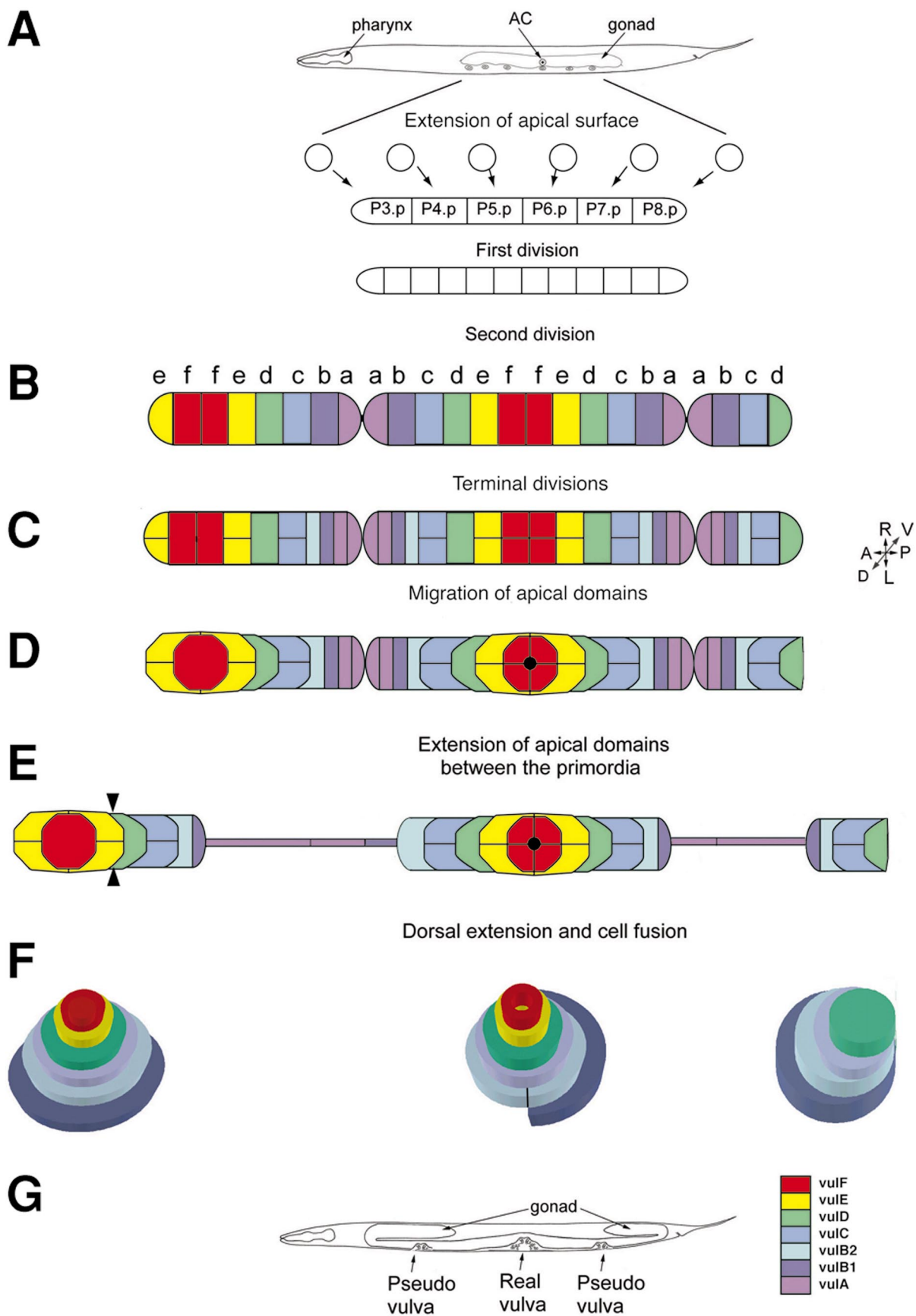
To study the development of the *let-60(n1046)* mutant vulva as well as the pseudovulvae that are characteristic of this *gf* mutant, we followed vulvae formation in living *n1046* worms expressing MH27-GFP (see Materials and Methods). In addition, we have stained worms from different stages of development with an antibody against the adherens junctions and observed three-dimensional confocal section reconstructions (Sharma-Kishore *et al.*, 1999). By analyzing these intermediates it was possible to reveal the mutual influence that the “real” and pseudovulvae exert on each other and to learn about the minimal cellular events required for the completion of the successive developmental phases. Figure 2 shows the summary of events during vulval formation in *let-60(n1046)*.

Divisions of the Vulva Precursor Cells Reveal Asynchronous Vulval Development of Pseudovulvae in *let-60(gf)*

In wild-type worms, the sublineages of the different VPCs are invariant and dependent on combined signaling pathways (Sulston and Horvitz, 1977; Horvitz and Sulston, 1980; Kimble, 1981; Euling and Ambros, 1996) (Fig. 1). In the *let-60(n1046sd)* *gf* mutant it has been shown that the induction signal gives rise to various sublineages resulting in the formation of ectopic pseudovulvae (Beitel *et al.*, 1990).

To investigate the morphogenesis derived from these abnormal sublineages in *let-60(n1046)*, we have analyzed living worms and reconstructed intermediates from the mid-L3 stage, 29–33 h posthatching (Fig. 3). During the first round of the VPC's division in *n1046* mutants, the spatial and temporal pattern of the division of P(3-8).p was indistinguishable between the different VPCs. However, during

FIG. 2. Multivulva formation in the *let-60(n1046)* *gf* mutant. (A–C) P(3-8).p adopt different cellular fates according to the signals from the surrounding cells as well as a Let-60/Ras ectopic signal that is a result of a *gf* mutation (Eisenmann and Kim, 1997). This is one of the observed fates of the VPCs in *let-60(n1046)* and is represented also in Figs. 4 and 5. (B) All the VPC's daughter cells divide longitudinally. (C) During the terminal round of division the anterior pseudo f cells did not divide in this example. (D) Real and pseudovulvae precursor cells migrate toward their respective primordia midlines as in wild-type animals (Fig. 1) except for the fact that the furthestmost cells attached between the different primordia stretch due to competitive attractiveness between equidistant primordia. The f cells in the anterior pseudovulva fuse. (E) The daughters of a in all the primordia and the anterior b1 in the real vulva primordium do not complete their migrations and are therefore absent from the evolving vulvae. As a result, the primordia are asymmetric. In the absence of their symmetrical pairs, two filopodia (arrowheads) migrate toward the midline and turn toward each other until they meet, producing concentric toroids and forming a stack of only five or six rings. (F) The extended cells between the primordia either fuse to *hyp7* (as in this example) or remain throughout vulvae formation. Newly formed rings undergo a temporal and spatially ordered process of intratoroidal fusions. The real vulva becomes mature and functional although part of its normal distal components are missing. Specific cells can adopt the structural differentiated states of the absent cells as a result of cell fate transformation. See text for details. (B–E) are dorsal views; (A and G) are lateral views. AC, anchor cell (black dot in D and E). A, anterior; P, posterior; R, right; L, left; V, ventral; D, dorsal.



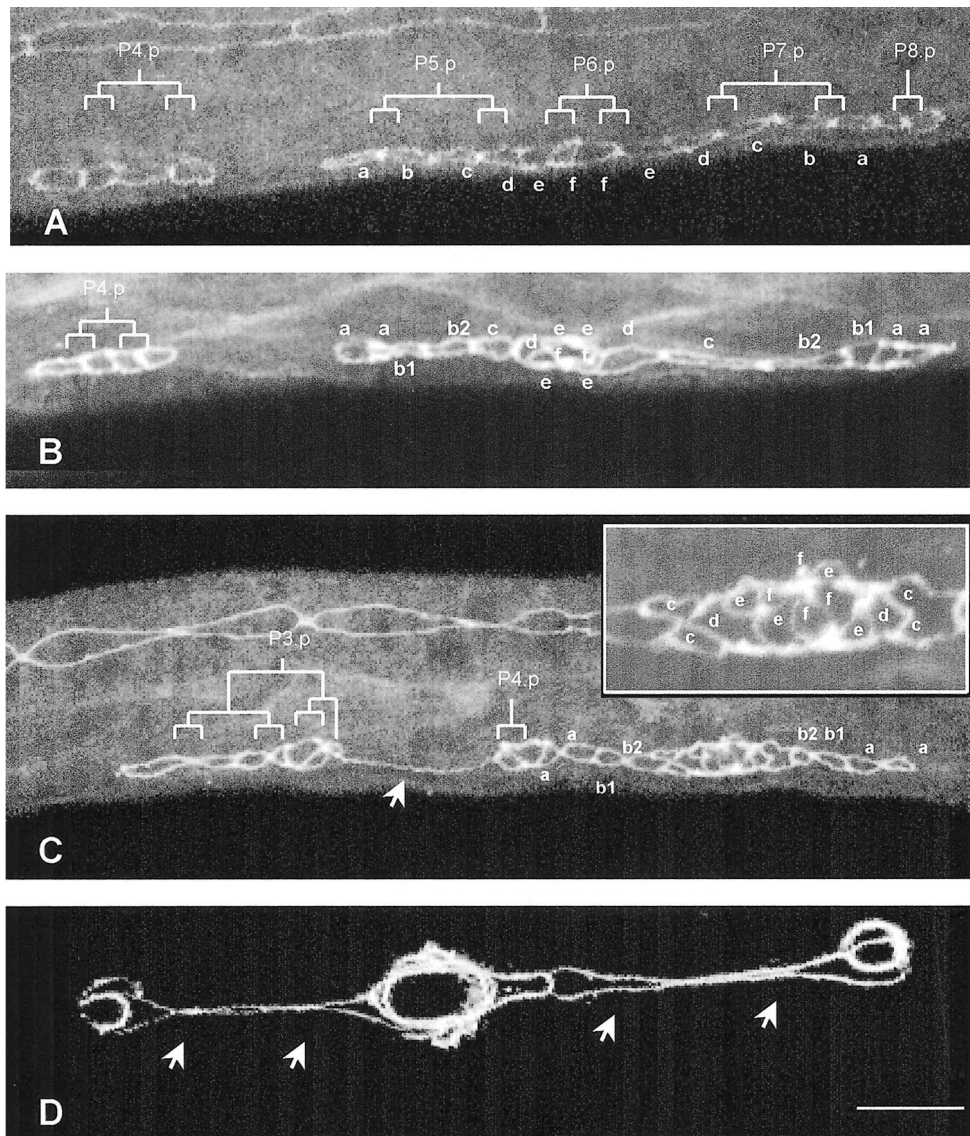


FIG. 3. Heterochronic proliferation of VPCs. Confocal micrographs of mid-L3 to mid-L4 vulvae stained with MH27 mAb (A–C) that reveal adherens junctions (Francis and Waterston, 1991; Podbilewicz and White, 1994) or vulvae expressing an MH27-GFP construct in their apical junctions. (D). Pictures were obtained by projecting 5–10 serial confocal sections of $0.5 \mu\text{m}$. (A) Early primordia with the 12 granddaughters of P(5–7).p after two rounds of cell division (a–f and f–a) as well as the granddaughter cells of P4.p and the daughter cells of P8.p (approximately 31.5 h posthatching). (B) Primordial cells of an asymmetrical real vulva during the terminal round of division (32.5 h). P4.p has undergone only two rounds of divisions yielding four granddaughter cells and the daughter cells of P8.p have fused to *hyp7* (h fate; 3° sublineage). (C) Beginning of short-range migrations: the descendants of P3.p and P(5–7).p during the terminal round of division. P4.p has divided only once (34 h). (Inset) A higher magnification of the center of the real vulva primordium showing the great-granddaughters of the VPCs. Arrow points to the filopodia that links two primordia. (D) A real and two pseudovulvae after ring formation. Arrows indicate extended cells between the primordia. These cells do not complete their migrations and will not participate in the formation of the vulvae. In all the pictures anterior is to the left. Bar, $10 \mu\text{m}$. Estimated times are in hours post hatching and are based on Nomarski optics and stage of development of the seam cells (see A and C, above the vulval cells).

the second round of division, the daughters of P3.p, P4.p, and P8.p, which did not fuse to *hyp7* (3° sublineage), divided asynchronously (Fig. 3; G. Shemer and B. Podbilewicz, unpublished data).

The 12 cells of wild-type animals (a–f and f–a) undergo a terminal round of division at this stage (see legend to Fig. 1B). In *n1046*, P(5–7).p and their progeny divided temporally and spatially in a similar way to the wild type but the

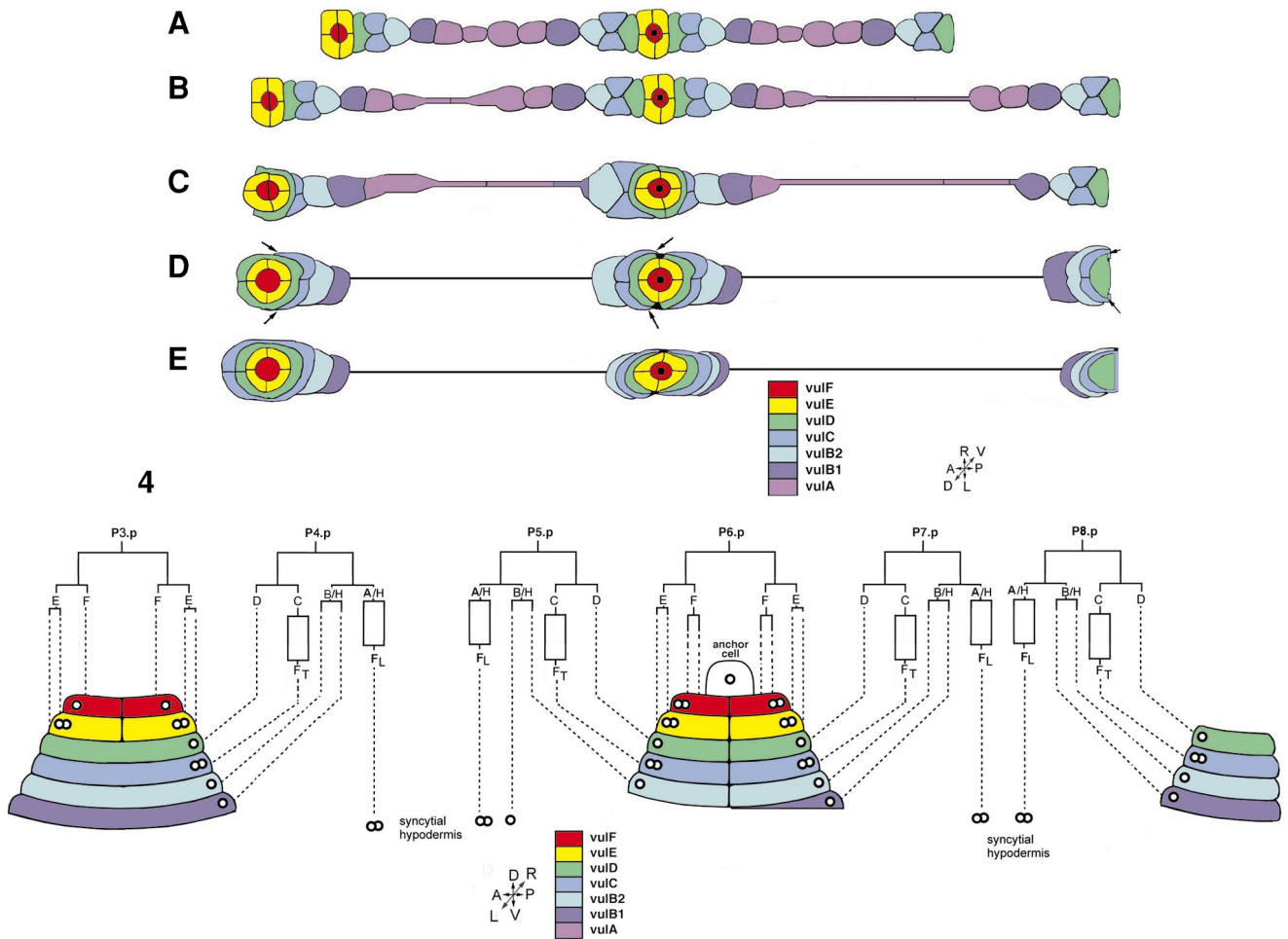


FIG. 4. Early morphogenesis of vulval cells Apical junctions of the cells were visualized and pictures were obtained as described in Fig. 3. The schematic drawings are dorsal views based on these pictures. (A) Intermediate with all 22 vulval cells plus 13 primordial cells of the anterior pseudovulva and 7 cells that form the primordium of the posterior pseudovulva. (B) The different primordia began to invaginate while the most external cells of the primordia have extended their apical surfaces. (C) In the real vulva, vulD precursors have migrated to surround the inner rings of vulE and vulF. In the anterior pseudovulva primordium vulD precursors have migrated toward their inner neighbors and, in the absence of symmetrical pairs, have encompassed vulE and vulF. The extended daughter cells of a have fused in all the different primordia. In the real vulva the anterior b1 cell has also extended. (D) In the posterior pseudovulva, vulC precursors have sent extensions (arrows) surrounding vulD that in the absence of vulF served as the inner “organizer” cell. In the absence of symmetrical pairs, these extensions turned toward each other. Similar filopodia are shown in the anterior pseudovulva and in the central real vulva (arrows). (E) vulC precursors in all the primordia have fused in pairs in a transverse fusion. In the real vulva the vulC ring has formed. In the anterior primordium, these fused cells have sent processes that have encompassed the inner rings. In the posterior primordium, the vulC ring has formed after the apical extensions had met and fused. Closed black circle at the center of the real vulva represents the AC that invades and penetrates the four vulF precursor cells.

FIG. 5. Cellular fates and structural differentiated states of the primordial cells of the vulvae. A schematic representation of mid-L4 vulvae (~38 h) based on fixed and live worms showing the stacks of rings before intratoroidal fusions. The lineage relationships of the different rings are indicated. The cell fates are indicated by the ring precursors (A–F) or by cells that will not participate in vulvae formation (H). In the anterior pseudovulva the descendants of P3.p and P4.p have formed a stack of six rings (vulE-like and vulF-like, 1° sublineage of P3.p; pseudo-vulB1-vulD, 2° sublineage of P4.p.). In the posterior pseudovulva four rings, half in size of normal rings, have been formed (pseudo-vulB1-vulD, 2° sublineage of P8.p as shown before). The real vulva is composed of only five complete rings and one half-ring (the posterior vulB1). Timing of division between the VPCs is only schematic as division status of the different VPCs is variable. The open rectangles represent cell fusion. Open circles represent nuclei. Free nuclei represent cells that have fused with the hypodermal cell hyp7. FL, longitudinal fusion; FT, transverse fusion.

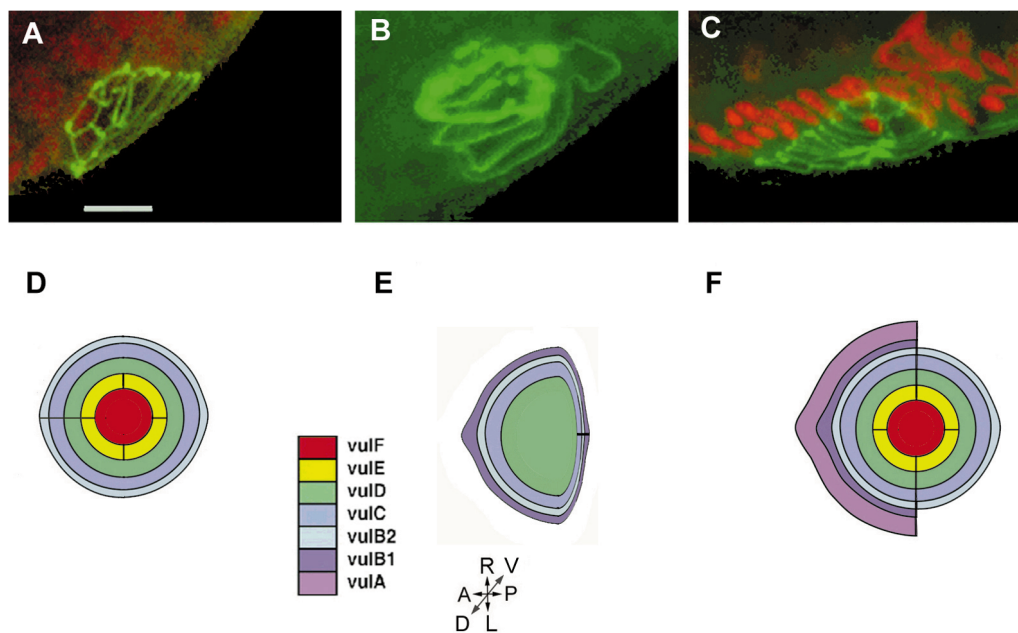


FIG. 6. Ring formation in pseudovulvae. Pictures of confocal reconstructions (A–C) and their respective dorsal view diagrams (D–F) of pseudovulvae prior to intratoroidal fusion stained with MH27 mAb (adherens junctions, green) and propidium iodide (nuclei, red). Nuclei of vulval cells were distinguished from the rest of the cells by analysis of each section. The identity of the rings is based on the structural resemblance to known rings in the wild type (see Materials and Methods). (A and D) Pseudovulva containing pseudo vulB2–vulF. The three most ventral rings have each formed from only one half-primordium. vulF is formed from two f cells that fuse between themselves. (B and E) Pseudovulva containing only four rings, each of them formed from only one half-primordium. The d cell has served as the inner “organizer” cell. (C and F) Pseudovulva containing seven anterior half-rings and five posterior half-rings. This pseudovulva contains 13 nuclei suggesting that the descendants of P3.p and P4.p acted together to obtain this structure not in the conventional way of adopting a 1° or a 2° sublineage. The cells in rings vulA–vulE have not achieved cell fusion and we would expect them to fuse before the L4 to adult molt. All pictures with ventral down and anterior to the left. All pseudovulvae are from animals in the mid- to late L4 stage. Bar, 10 μ m.

progeny of P3.p, P4.p, and P8.p showed again, like in the 12 cells stage, a retarded phenotype (Fig. 3B). In 28% of the cases P3.p, P4.p, and P8.p divided three times like P(5–7).p yielding 7 or 8 great granddaughter cells (2° or 1° sublineage, respectively) depending on their pattern of division (e.g., P3.p in Fig. 3C). However, in 72% of the cases the extra cells divided only once or twice while P(5–7).p had divided three times (e.g., P4.p in Fig. 3B). The extra cells that escaped the 3° sublineage (fusion to *hyp7*) were either linked or not linked to the real vulva primordium regardless of their division status (e.g., Figs. 3A–3C). This phenomenon was also observed in later stages of development leading us to conclude that the transformed VPCs can divide at a slower rate than the descendants of P(5–7).p and that some transformed VPCs divide only once like in the wild type but escape fusion to *hyp7*.

Short-Range Migrations: Competition between Migrating Cells

In wild-type *C. elegans* the next stage of vulva development is characterized by short-range migrations that involve the extension of apical domains between equivalent

cells from the two sides of the vulva primordium toward the center (Figs. 1C and 1D).

To analyze cell migration in *let-60(n1046)*, we have investigated living worms and reconstructions of migration intermediates (33–36 h post hatching). We found that in each primordium the cells migrated toward their primordium’s midline but at the onset of the migrations, the apical domains of the most external cells elongated abnormally forming apical extensions between the different primordia (Figs. 2E, 3C, and 3D, arrows). These apical extensions were observed in all of the worms investigated from the beginning of the short-range migrations until later stages. The elongated cells either fused later to *hyp7* (Fig. 2F) or remained throughout the entire vulvae formation (Fig. 3D).

One interpretation of the apical extensions is that they represent competition between the different primordia during cell migration. To understand how this competition affects the resulting real and pseudovulvae, we characterized the primordia of intermediates from the early and mid-L4 stage, after the completion of these short-range migrations. The precursors of vulE–vulB2 migrated normally in all the real vulvae primordia. However, the A cells (and sometimes also the B1 cell) had not completed their

TABLE 1
Asymmetry between the Two Halves of Real Vulvae

| Ring status ^a | % of total semivulvae (n = 42) |
|---|--------------------------------|
| No vulA | 40% (17) |
| No vulA + no vulB1 | 29% (12) |
| Incomplete migration of vulA primordial cells | 29% (12) |
| All rings exist | 2% (1) |

^a Half-primordia were counted and the state of the migration of their precursors was determined. Half-primordia that lacked specific rings were calculated as percentage of the total half-primordia observed. In parentheses are numbers of half-primordia.

short-range migrations or had not migrated at all. In both cases the result was the absence of these cells from the mid-L4 primordia (Table 1, Figs. 4, 5, and 7C). Only in 1 case of 42 did all of the half-rings' precursors seem to have completed their migrations. In all of the cases analyzed where there were no extra cells near the real half-vulvae (when the P8.p cells executed the 3° sublineage), the short-range migrations were not slowed down. This is consistent with the competition between the extra cells that did not fuse to *hyp7* and the real vulva cells (Fig. 4).

In Fig. 4, pseudovulvae were either formed from the descendants of one VPC (P8.p) or two VPCs (P3.p and P4.p). The migration pattern of the pseudoprimordia resembled that of the real primordium. Both involved sending apical processes from the outer cells toward the inner cells with the concomitant remodeling of adherens junctions with *hyp7*.

In summary, we found that real vulva cells and pseudovulvae cells of *n1046* migrated toward the vulva (or pseudovulvae) midline in the same manner as in the wild-type animals except for the most distal cells attached between the primordia, that did not migrate or did not complete their migration.

Autonomy of the Two Halves of the Vulva Primordium Results in Asymmetry in Size, Orientation, and Cells Content

Two halves derived from anterior and posterior cells form each ring in the wild-type vulva (Figs. 1D and 7A). To investigate whether cells attract each other or alternatively vulval cells behave autonomously, we have analyzed the formation of natural semivulvae composed of half-rings in *let-60(n1046)*. When looking on real vulvae in mid-L4 reconstructions and living worms expressing MH27-GFP, equal number of precursor cells in both halves was obtained only in cases where both halves were subjected to equal competition with nearby pseudovulvae (Figs. 7D and 7E). We observed that in most cases both halves showed A-P asymmetry with an unequal number of vulA and/or vulB1 precursor cells (Figs.

2, 4, 5, 7B, and 7C). This asymmetry was not confined to the contents of the rings but also to their size and orientation. In 54% of these primordia, one half was larger than the other half (Fig. 7B). In addition, in 71% of the vulvae inspected ($n = 24$), the apical domains were oriented toward the anterior side of the worm (arrowheads; Figs. 7D and 7E) regardless of the presence of a posterior pseudovulva primordium.

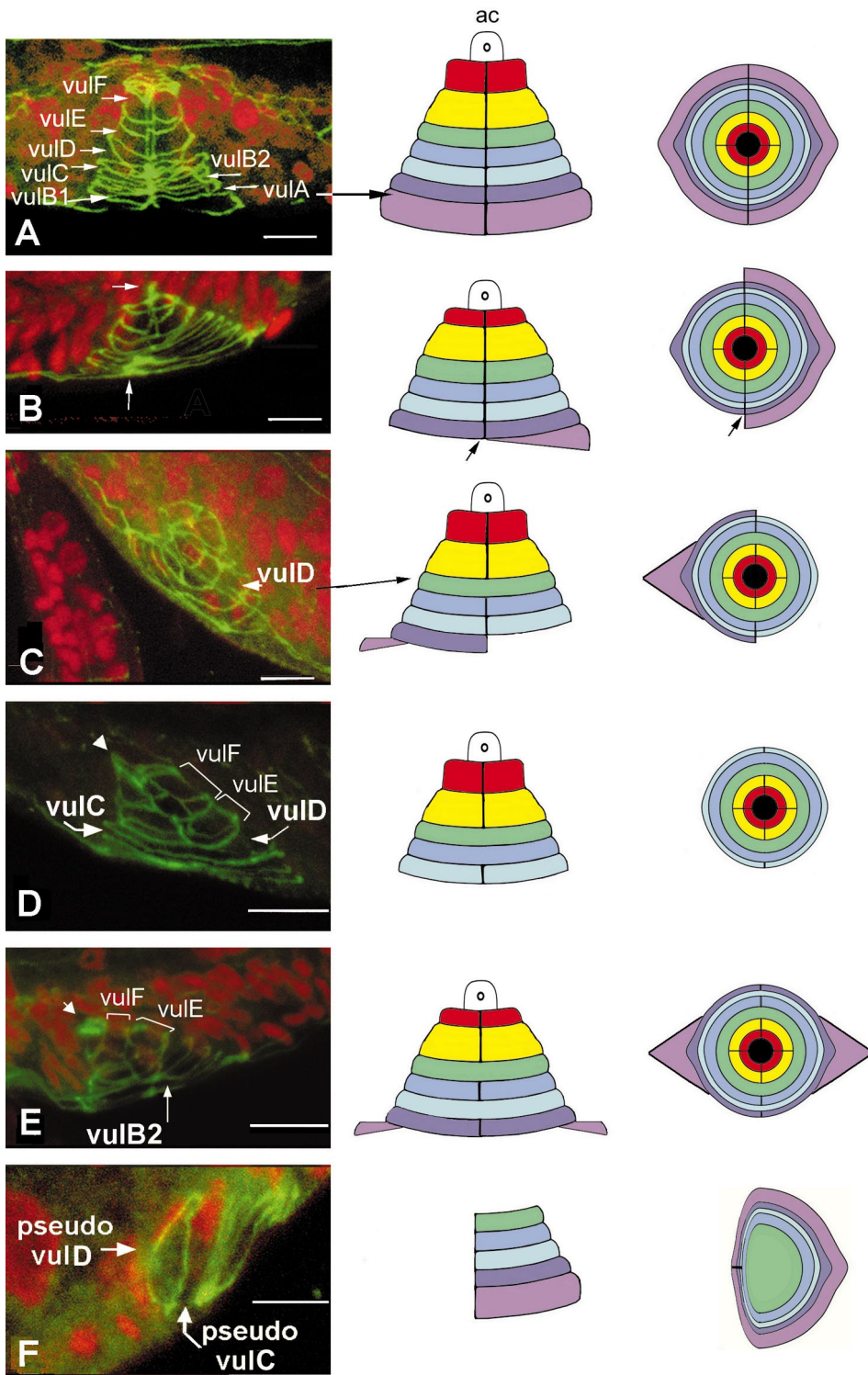
In summary, the asymmetry that we found in *let-60(n1046)* suggested that each half of the vulva developed autonomously. In the presence of nearby pseudovulvae, precursor cells of the two halves migrated unequally ending with an inclined invaginated primordium comprised of a different set of cells with additional structural asymmetries.

Ring Formation: Half-Vulvae Form "Self" Complete Rings

In wild-type *C. elegans* anterior and posterior pairs coordinately migrate to form rings (Fig. 1). To further study a natural situation of formation of half-rings in semivulvae and to analyze the process of invagination by ring formation step by step, we have examined pseudovulvae of *n1046* in fixed and living worms. The pseudovulvae we investigated can be divided into three main structural subclasses: (1) disorganized structures without any identified structural pattern; (2) pseudovulvae that developed a structure recognizable as those usually obtained by the 1° sublineage (pseudo vulE + vulF) or 2° sublineage (pseudo vulA-vulD; Figs. 6B, 6E, and 7F) or structures that are partially primary and partially secondary (Figs. 6A and 6D); and (3) complex structures with more rings than expected from the sublineage (Figs. 6C and 6F).

In 2° sublineage-derived structures, the cells sent two unidirectional extensions from outer to inner cells as the pseudo D cell served as the midline (Fig. 4C; posterior pseudovulva). In the absence of symmetrical pairs, the extensions moved toward each other until they met thus forming complete rings (Figs. 4D and 4E). Because only one cell (D) served as the midline (compared with four F cells in wild-type animals) the rings were half in size in their A-P axis of the normal ones (Figs. 2, 4, and 5; posterior pseudoprimordium; Figs. 6B, 6E, and 7F). When primordia of pseudovulvae adopted a more complex structural shape (partially vulE-vulF-like and partially vulA-vulD-like) that contained four or two pseudo F's, the outer cells formed complete and full-sized rings similar to the real vulva and to the vulva of wild-type animals. Here, also, the cells have sent apical extensions that turned toward each other in the absence of symmetrical pairs (Figs. 2, 4, and 5, anterior pseudoprimordium; and Figs. 6A and 6D). Thus, the size and shape of the A-D-derived rings is determined by the dimensions of the dorsal rings that formed first (vulF or vulD).

In summary, the ring asymmetry and the formation of



“self” rings indicate that cell migration and cell fusion are autonomous processes.

Transformations of Rings and Fusion Fates between the Vulval Toroids

Figure 5 shows the formation of incomplete stacks of rings due to the competition between primordia in *let-60(n1046)*. We propose that the ultimate cell fate of the VPCs descendants is a structural differentiated state expressed as the different rings. A to F represent the cell fate of ring formation and H represents the cell fate of fusion to *hyp7*.

Intratoroidal Fusions: Transformations of Cell Fusion Fates

In the wild-type, after all the primordial cells complete their migrations and during invasion of the AC followed by its fusion to the utse uterine cell, there is an ordered process of fusion within the rings starting with *vulD* and ending with *vulE* with the exception of *vulB1* and *vulB2* (Sharma-Kishore *et al.*, 1999). As a result, a stack of seven rings is built (Fig. 1) and this organ is attached to the surrounding epithelia (through processes from *vulE*), to *hyp7* (through *vulA*), to vulval muscles (Sharma-Kishore *et al.*, 1999), and to the uterus (Newman and Sternberg, 1996; Newman *et al.*, 1996). Figure 7A shows a wild-type vulva after ring formation and before intratoroidal fusion. In the wild-type vulva the order of the intratoroidal cell fusions are *vulD*, *vulA*, *vulC*, *vulF*, and *vulE* (Sharma-Kishore *et al.*, 1999).

In *n1046*, the precursor cells of *vulA* and *vulC* (A + A and C + C, respectively) fused between themselves on each side of the primordium before (*vulA*) and during (*vulC*) the migrations as occurs during early fusion events in the wild type (compare Figs. 1C and 1D with 4B–4E).

To investigate the intratoroidal fusions phase in *n1046*, we have analyzed reconstructed larvae and living worms

from the mid-L4 stage. We found that even after abnormal migrations, the process of intratoroidal fusions did take place. Figures 7C–7E show reconstructed vulvae in different stages of intratoroidal fusions. Like in the wild type, this phase started only after all the cells that do participate in the formation of the vulvae had completed their migrations (e.g., Figs. 7C and 7E). This suggests that the temporal order of events is independent of the components of the primordia but is dependent on the completion of the migration process by the participating cells.

In *n1046*, the two cells of *vulD* were the first to fuse longitudinally (Fig. 7C). In the absence of *vulA* from the primordia, the *vulC* cells fused next (Fig. 7D) and the normal order of events proceeded. In one reconstructed vulva lacking *vulA*, the two cells forming *vulB2* fused adopting the fate of *vulA* even though in the wild-type they do not fuse (Fig. 7E). The transverse intra-toroidal fusion (F_{IT}) in *vulF* sometimes were found early (e.g., Figs. 7B and 7C right diagrams) and in other cases they occurred after the longitudinal intratoroidal fusion (F_{IL}) as in the wild-type (e.g., Figs. 7D and 7E). As for the pseudovulvae, we observed intratoroidal fusion of pseudo *vulC* (*vulD*-like is composed of only one cell in this case) at least in one reconstructed intermediate (Fig. 7F). Thus, where A cells fuse to *hyp7*, the precursor cells of *vulB* accomplish a proper interface with *hyp7* allowing the base of the vulva to attach to the hypodermis (e.g., Figs. 2F, 5, 6A, and 7D).

To summarize, in the absence of specific cells in *n1046* the fusions within the existing rings took place after the participating cells of the primordium had completed their migrations. The fusions followed the same order as in the wild-type vulva with the exception of *vulA* that did not participate in vulva formation and the transverse fusions (F_{IT}) of *vulF* that were variable. In one case we detected substitution of the A cell fate by the descendants of the B cell not only in forming the most ventral ring (*vulB1*), but also in undergoing intratoroidal fusion (*vulB2*) (Fig. 7E).

FIG. 7. Intratoroidal fusion in real and pseudovulvae. Confocal reconstructions of vulvae from the mid- to late L4 stage stained as in Fig. 6. Left column, confocal reconstructions. Middle column, lateral view diagrams. Right column, dorsal view diagrams. (A) Wild-type vulva. (B–D) Real vulvae of *n1046*. (E) Pseudovulva of *n1046*. (A) Lateral view of a wild-type vulva where no intraring cell fusions have occurred. (B) Primordium containing six rings and one posterior half-ring. *VulF* fused transversely and the rings have not yet undergone intratoroidal fusion. Arrows point to midline where junctions between anterior and posterior vulval cells are. (C) Primordium in which *VulF* fused transversely and the *vulD* ring has undergone intratoroidal fusion as expressed by the disappearance of the boundaries between the cells comprising this ring. In the anterior half the *vulA* precursor cells have not completed their migration while in the posterior half these cells as well as *vulB1* precursors have not migrated at all and are absent from the primordium. (D) Primordium from later stages containing only five rings in which *vulC* has also undergone intratoroidal fusion. Arrowhead points to the apex of the stack of rings showing the orientation of the vulva toward the anterior side (left). (E) Primordium in which *vulB2* has undergone intratoroidal fusion (in addition to *vulD*) in the absence of the A cells that have not completed their migration. *vulB2* does not fuse in the wild type. Arrowhead dorsal of the stack of rings points to the asymmetric orientation of the vulva toward the anterior side. (F) Primordium of a posterior pseudovulva containing five complete rings in which the pseudo *vulD* cell serves as the most dorsal ring. Pseudo *vulC* has undergone intratoroidal fusion. In the mutant *let-60(n1046)* the order of intratoroidal longitudinal fusions (F_{IL}) are unfused ($n = 6$), *vulD* ($n = 12$), *vulC* ($n = 5$), and *vulF* and *vulE* ($n = 1$). The order of transverse intratoroidal fusions (F_{IT}) for *vulF* is variable since F_{IT} have been found associated with different stages of F_{IL} fusions ($n = 6$). In the wild type the order is *vulD*, *vulA*, *vulC*, *vulF*, and *vulE*. For the two most dorsal rings, F_{IT} and F_{IL} events are coupled in the wild type but not in the mutant. All pictures with ventral down and anterior to the left. Bar, 10 μ m. ac, anchor cell (black dot).

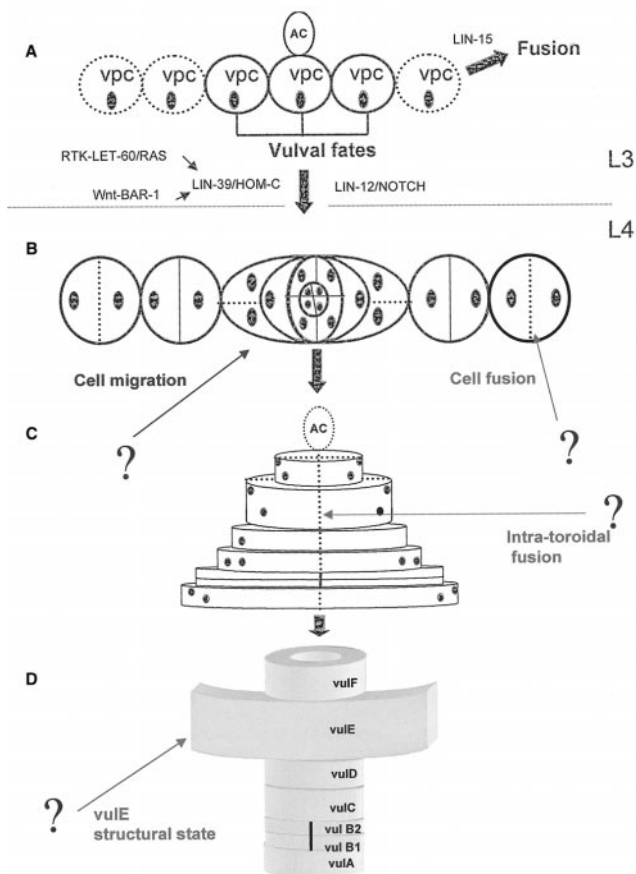


FIG. 8. A working model for the cell behaviors that drive invagination of the vulva. (A) During the L3 stage the AC induces three of the six multipotential VPCs to adopt vulval fates with the involvement of RTK-LET-60/RAS and Wnt-BAR-1 signaling pathways (Eisenmann *et al.*, 1998; Han *et al.*, 1990; Lackner *et al.*, 1994). LIN-12 is a receptor for the LIN-12-Notch family that is required for lateral signaling (Greenwald *et al.*, 1983) and LIN-15 induces cell fusion or inhibits vulval fates (Herman and Hedgecock, 1990; Thomas and Horvitz, 1999). (B) Based on our work on vulva morphogenesis in wild-type and *ras/let-60* hermaphrodites we propose that additional signaling pathways are involved in stereotyped autonomous cell migration and cell fusion processes during ring formation in the late L3 and early L4 stages. (C) After the seven rings are formed intratoroidal fusions occur in a regulated way and the AC fuses to the uterine cells. It is unknown how this process is controlled. The seven rings show a pyramidal shape before and during intratoroidal cell fusions. (D) Morphological changes determine the seven structural differentiated states (vulA-vulF) and the shape of the stacked rings become cylindrical instead of pyramidal. This transverse view also shows the structural differentiated state of vulE that undergoes a major expansion after the intratoroidal fusion step linking two basolateral domains to the lateral hypodermal seams cells (see also Fig. 1F). RAS and other signaling pathways as well as specific fusogenic molecules may be involved in the different steps shown here (?). Fusing membranes (dotted lines). Nuclei (black circles).

Last Phase of Vulva Formation

During this phase that involves vulva eversion followed by lumen closure, we have not seen any difference between the development of the real vulva of the mutant and the wild-type vulva. As for the pseudovulvae, this phase did not involve closure of the lumen since no lumen was opened in the absence of the AC.

DISCUSSION

We have done a step-by-step analysis of vulvae formation in a *ras/let-60* Muv mutant through investigation of reconstructed intermediates from different stages of development as well as using a GFP-tagged adherens junction marker enabling us to better understand the minimal requirements for each of the developmental cellular events. The sequence of events leading to the real and pseudovulvae in this mutant is summarized in Fig. 2. We have also described the mutual relationships between the different vulvae and arrived to three major conclusions: (1) The different primordia compete between themselves for vulval cells. (2) Each half-primordium develops autonomously. (3) The ultimate fate of each vulval cell is to become one of the seven structural cell types that comprise the vulva.

The Primordial Cells of the Most Dorsal Ring Have a Key Role in the Migration Stage

On the onset of vulva formation, the primordial cells have apparently "divided" into groups according to their future structural differentiated state (forming a real or a pseudovulva). The pattern of morphological events leading to vulva formation was similar between these groups (Figs. 2 and 3). Two events are crucial for the development of the vulvae. The first event is the determination of a primordium's midline, toward which the outer cells migrate. Our results suggest that the boundaries between the primordial cells of the most dorsal ring vulF may be the default midline as the outer cells migrated toward these boundaries not only in the wild-type vulva or the real vulva in *let-60(n1046)*, but also in pseudovulvae that contained pseudo-vulF (Figs. 4, 6A, 6C, 6D, and 6F). In other cases, the precursors of the most dorsal ring acted similar to the pseudo vulF and served as a midline (e.g., Figs. 6B, 6E, and 7F). The second event is the trigger that starts the short-range migrations. Evidence for the existence of this trigger came from the putative competition between the primordia in this Muv mutant. Although each group of cells acted as an independent primordium, the presence of nearby groups affected them and the most external cells did not complete their migration. It is possible that these cells were subjected to signals from both midlines and "could not decide" where to migrate to, suggesting that cells that serve as a midline are critical in determining the normal temporal and spatial order in which the cells migrate. These results suggest that the primordial cells that form the most dorsal ring (vulF in

the real vulva) play a key role in the onset and throughout the short-range migrations stage. When the F and E cells are absent then D cells become the “organizer”. We propose that there is a hierarchy A to F and each cell knows to migrate toward a neighbor that is higher in the sequence (A, B1, B2, C, D, E, F).

Each Half-Vulva Develops Autonomously

Vulvae formation in the *ras/let-60* mutant described here has enabled us to follow the behavior of many half-vulvae during each and every stage of development. Our results establish that each half-vulva develops autonomously throughout vulva organogenesis. First, due to the competition between the different primordia (see above), each half of the real vulva developed differently leading to asymmetrical vulvae (e.g., Figs. 4, 7B, and 7C). Second, in pseudovulvae that lacked half of the primordial cells, the existing cells started migrating, turned toward themselves after the midline had been passed, and fused intratoroidally forming complete rings (Figs. 4 and 7F). Thus, the correct sequence of events is independent of the interactions between the symmetrical halves. Each half-primordium develops independently over a limited time range and for a defined set of cell migration and cell fusion events. For example, in cases when one half-primordium contributes E/F fates and the other half-primordium contributes A/D fates, the E/F become the organizer and set the center. D cells then migrate and surround vulE/vulF rather than competing for the center (G. Shemer and B. Podbilewicz, unpublished results). Previous work on the wild-type vulva has shown that each half-vulva can develop autonomously (Sharma-Kishore *et al.*, 1999). However, this report was based largely on only one observation of an EM reconstructed late L4 vulva that had undergone laser microsurgery killing the posterior half of the vulva and on cell lineaging evidence from early stages of vulva formation, prior to organogenesis. Viewing the results presented here, we suggest that key players in the regulation of ring formation are the primordial cells of the most dorsal ring and the surrounding hypodermal syncytium. In addition, the developmental pattern of half-pseudovulvae implies that the cells are intrinsically activated resulting in their ability to migrate until they find “self,” stop migrating, and undergo intratoroidal fusion even in the absence of their symmetrical pairs (Fig. 4). However, when two half-primordia produce sets of homologous cells, the homologues will eventually recognize each other and extend arms toward each other in a somewhat coordinated fashion, even if the final product ends up asymmetric. Thus, the two halves interact and maintain a hierarchy of cell fates and when one half is missing cell migration, cell fusion and ring formation occur autonomously without changing the F to A center to periphery and dorsoventral hierarchy of interactions.

Cellular Fate versus Structural Differentiated State

Previous work has described in detail the cellular sublineages of the VPCs (Sternberg and Horvitz, 1989; Greenwald,

1997). The VPCs undergo a stereotyped sequence of cell divisions (1°, 2°, and 3° sublineages) that result in seven cell fates (A, B, C, D, E, F, and H; Figs. 1A, 2B and 5). Thus, the cellular sublineage is followed by seven cell fates of which A–F fates will form vulval rings (Sharma-Kishore *et al.*, 1999). In the wild type the tube-shaped vulva is formed from a stack of seven rings (seven structural differentiated states), some of them multinucleated (Fig. 1) (Sharma-Kishore *et al.*, 1999). However, in *let-60(n1046)*, although some of the VPCs have not changed in their cellular sublineage (P(5-7).p), their structural differentiated state was completely different (Figs. 2, 5, 6C, and 7E). We propose to distinguish between the cellular fates and structural differentiated states by the following nomenclature: A–F (cell fates) for precursors of vulA–vulF (structural differentiated states), respectively, and H (cell fusion fate) for cells that will not participate in vulva formation and may fuse later to the surrounding hypodermis.

Inhibiting Proliferation and Promoting Fusion of VPCs May Be Separate Processes

The descendants of P3.p, P4.p, and P8.p do not always proliferate at the same rate as those of P(5-7).p (Fig. 3; G. Shemer and B. Podbilewicz, unpublished data). In fact, we observed cases where one of the VPCs divided only once and the two daughter cells remained undivided until vulva formation had been completed. According to the 3° sublineage (H cell fate), a single division of a VPC should result in fusion to *hyp7*. However, these cells have escaped this fate, suggesting that fusion to *hyp7* is not a default process following proliferation arrest of VPCs daughter cells but rather that cell fusion and proliferation are two separate processes. Previously, it has been shown that the 3° cellular fate appears to be the result of an intracellular signaling system between *hyp7* and the VPCs and that two classes of genes are needed to inhibit vulval cell fates (Ferguson and Horvitz, 1989; Herman and Hedgecock, 1990; Hedgecock and Herman, 1995; Thomas and Horvitz, 1999). It is still not well understood how these pathways actually work. The ectopic activity of RAS/LET-60 in *n1046* may bypass the fusion–promotion pathway leading to nonproliferating cells that escape fusion.

A Novel Potential Role for RAS in Vulva Organogenesis

The function of the RAS protein is not limited to its central role in proliferation. It has been previously shown that RAS is not essential for general proliferation in *C. elegans* and *Drosophila* (Hou *et al.*, 1995; Yochem *et al.*, 1997). However, RAS and other small-related GTPases have been shown to play key roles in axon guidance (Zipkin *et al.*, 1997), spicule formation, germ cell development (Yochem *et al.*, 1997), and sex myoblast migration (Clark *et al.*, 1992) in *C. elegans*, eye development (Wassarman *et al.*, 1995), embryonic patterning (Schnorr and Berg, 1996), and

wing vein formation (Roch *et al.*, 1998) in *Drosophila* and motility, as well as invasiveness of various mitogenic cells in mammals (Keely *et al.*, 1999). In the vulva the only evidence for RAS participation in the actual morphogenesis is the EGF reciprocal signaling that is important for establishing the uterine–vulva connection (Chang *et al.*, 1999).

Our results imply that RAS may have a potential role during the entire organogenesis of the vulva in cell fusion and cell migration. First, in the background of a *ras* (*gf*) mutation, at least some of the cells (the daughters of A in the real vulva) have acquired the ability to fuse to the surrounding hypodermis. The early inductive function of RAS could not contribute to this phenomenon since the lineage of these cells was normal. Rather, this mutation affects the cell fate of A. Second, in the *let-60/ras* (*gf*) mutant there are abnormal filopodial extensions of A- and B-derived cells (e.g., Figs. 2E, 3C, 3D, and 4). Third, the structural differentiated state transformation described may be related to the RAS pathway since RAS is normally expressed in all the primordial cells after the execution of the sublineage and throughout vulva formation (Dent and Han, 1998). Based on these results we propose that RAS and other signal transduction processes are involved in late cellular events (e.g., filopodial extensions and cell fusion) required to form a stack of rings that drive invagination (Fig. 8).

It has been shown that FUS3, a member of the RAS-MAP kinase pathway, is involved in the fusion of yeast cells during mating (Elion *et al.*, 1990). Cell fusion is also critical in fertilization (Yanagimachi, 1988), formation of epithelia in *C. elegans* (Podbilewicz and White, 1994), embryonic development in sea urchin and in leech (Hodor and Ettensohn, 1998; Isaksen *et al.*, 1999), and formation of muscles (Doberstein *et al.*, 1997), bones (Jee and Nolan, 1963), and placenta (Pierce and Midgley, 1963). Our working hypothesis is that membrane fusion during development is a universal strategy to accomplish pattern formation (Podbilewicz, 2000).

Ring Formation as a Morphogenetic Force in Invagination

Epithelial invagination plays a key role during developmental events such as gastrulation and organogenesis. There are various theories on the mechanisms and the morphogenetic forces that drive epithelial invagination such as apical constrictions in the ventral furrow in *Drosophila* as well as in the primordia of the neural crest (Schoenwolf and Smith, 1990), changes in cell adhesion properties of the basal and apical domains of the folding cells (Gustafson and Wolpert, 1963), secretion of extracellular matrix (Lane *et al.*, 1993), and oriented cell division during gastrulation (Hertzel and Clark, 1992). One of the candidates to be a morphogenetic force during invagination is the formation of bottle cells in sea urchin, *Drosophila*, and *Xenopus* embryos (Shih and Keller, 1994). These cells are apparently essential for primary invagination on the

onset of gastrulation (Kimberly and Hardin, 1998). Vulva formation in *C. elegans* has been studied in order to investigate the essence of epithelial invaginations in this animal and mutations that perturb vulva invaginations have been cloned (Herman *et al.*, 1999; Herman and Horvitz, 1999).

Here, we have shown that epithelial invagination during vulva formation in *C. elegans* can be executed through a novel mechanism. Ring formation appears to be the morphogenetic force that drives the invagination of the vulval cells. Invagination is achieved when cells forming rings migrate laterally and ventrally thus disconnecting neighboring cells from the hypodermis. We propose that sequential migration and ring formation is followed by interactions between the migrating cells and between the toroidal cells and the surrounding hypodermis. When ring formation is aberrant, invagination is not complete. It is noteworthy that the bottle cells in sea urchin are also set in a ring but that the folding of these cells is quite different from the process of ring formation in *C. elegans*.

ACKNOWLEDGMENTS

We thank J. White, D. Gershon, T. Gattegno, and M. Glickman for valuable discussions and two anonymous reviewers for their critical and constructive comments on the manuscript. We thank B. Mohler, J. Simske, and J. Hardin for strain jcls1. Some nematode strains used in this work were provided by the *Caenorhabditis* Genetics Center, which is funded by the NIH National Center for Research Resources. This work was supported by the Jacob and Rosaline Cohn Academic Lectureship and by grants from the Israel Science Foundation, the Israel Cancer Research Fund (U.S.A.), and the Binational Science Foundation (Israel).

REFERENCES

- Beitel, G. J., Clark, S. G., and Horvitz, H. R. (1990). *Caenorhabditis elegans* *ras* gene *let-60* acts as a switch in the pathway of vulval induction. *Nature* **348**, 503–509.
- Brenner, S. (1974). The genetics of *Caenorhabditis elegans*. *Genetics* **77**, 71–94.
- Chang, C., Newman, A. P., and Sternberg, P. W. (1999). Reciprocal EGF signaling back to the uterus from the induced *C. elegans* vulva coordinates morphogenesis of epithelia. *Curr. Biol.* **9**, 237–246.
- Clark, S. G., Stern, M. J., and Horvitz, H. R. (1992). *C. elegans* cell-signalling gene *sem-5* encodes a protein with SH2 and SH3 domains. *Nature* **356**, 340–344.
- Dent, J. A., and Han, M. (1998). Post-embryonic expression pattern of *C. elegans* *let-60 ras* reporter constructs. *Mech. Dev.* **72**, 179–182.
- Doberstein, S. K., Fetter, R. D., Mehta, A. Y., and Goodman, C. S. (1997). Genetic analysis of myoblast fusion: *blown fuse* is required for progression beyond the prefusion complex. *J. Cell Biol.* **136**, 1249–1261.
- Eisenmann, D. M., and Kim, S. K. (1997). Mechanism of activation of the *Caenorhabditis elegans* *ras* homologue *let-60* by a novel, temperature-sensitive, gain-of-function mutation. *Genetics* **146**, 553–565.

- Eisenmann, D. M., Maloof, J. N., Simske, J. S., Kenyon, C., and Kim, S. K. (1998). The β -catenin homolog BAR-1 and LET-60 ras coordinately regulate the hox gene *lin-39* during *Caenorhabditis elegans* vulval development. *Development* **125**, 3667–3680.
- Elion, E. A., Grisafi, P. L., and Fink, G. R. (1990). *FUS3* encodes a *cdc2*⁺/CDC28-related kinase required for the transition from mitosis into conjugation. *Cell* **60**, 649–664.
- Euling, S., and Ambros, V. (1996). Heterochronic genes control cell cycle progress and developmental competence of *C. elegans* vulva precursor cells. *Cell* **84**, 667–676.
- Ferguson, E. L., and Horvitz, H. R. (1989). The multivulva phenotype of certain *Caenorhabditis elegans* mutants results from defects in two functionally redundant pathways. *Genetics* **123**, 109–121.
- Ferguson, E. L., Sternberg, P. W., and Horvitz, H. R. (1987). A genetic pathway for the specification of the vulval lineages of *Caenorhabditis elegans*. *Nature* **326**, 259–267.
- Finney, M., and Ruvkun, G. (1990). The *unc-86* gene product couples cell lineage and cell identity in *C. elegans*. *Cell* **63**, 895–905.
- Francis, G. R., and Waterston, R. H. (1991). Muscle cell attachment in *Caenorhabditis elegans*. *J. Cell Biol.* **114**, 465–479.
- Greenwald, I. (1997). Development of the Vulva. In “*C. elegans II*” (D. Riddle, T. Blumenthal, B. Meyer, and J. Priess, Eds.), Vol. 33, pp. 519–541. Cold Spring Harbor Laboratory Press, Cold Spring Harbor, NY.
- Greenwald, I. S., Sternberg, P. W., and Horvitz, H. R. (1983). The *lin-12* locus specifies cell fates in *Caenorhabditis elegans*. *Cell* **34**, 434–444.
- Gustafson, T., and Wolpert, L. (1963). The cellular basis of morphogenesis and sea urchin development. *Int. Rev. Cytol.* **15**, 139–412.
- Han, M., Aroian, R. V., and Sternberg, P. W. (1990). The *let-60* locus controls the switch between vulval and nonvulval cell fates in *Caenorhabditis elegans*. *Genetics* **126**, 899–913.
- Han, M., and Sternberg, P. W. (1990). *Let-60*, a gene that specifies cell fates during *C. elegans* vulval induction, encodes a *ras* protein. *Cell* **63**, 921–931.
- Hedgecock, E. M., and Herman, R. K. (1995). The *ncl-1* gene and genetic mosaic of *Caenorhabditis elegans*. *Genetics* **141**, 989–1006.
- Herman, R. K., and Hedgecock, E. M. (1990). Limitations of the size of the vulval primordium of *Caenorhabditis elegans* by *lin-15* expression in surrounding hypodermis. *Nature* **348**, 169–171.
- Herman, T., Hartwig, E., and Horvitz, H. R. (1999). *sqv* mutants of *Caenorhabditis elegans* are defective in vulval epithelial invagination. *Proc. Natl. Acad. Sci. USA* **96**, 968–973.
- Herman, T., and Horvitz, H. R. (1999). Three proteins involved in *Caenorhabditis elegans* vulval invagination are similar to components of a glycosylation pathway. *Proc. Natl. Acad. Sci. USA* **96**, 974–979.
- Hertzel, P. L., and Clark, W. H. J. (1992). Cleavage and gastrulation in the shrimp *Sicyonia ingentis*: Invagination is accompanied by oriented cell division. *Development* **116**, 127–140.
- Hodor, P. G., and Etensohn, C. A. (1998). The dynamics and regulation of mesenchymal cell fusion in the sea urchin embryo. *Dev. Biol.* **199**, 111–124.
- Horvitz, H. R., and Sulston, J. E. (1980). Isolation and genetic characterization of cell-lineage mutants of the nematode *Caenorhabditis elegans*. *Genetics* **96**, 435–454.
- Hou, X. S., Chou, T. B., Melnick, M. B., and Perrimon, N. (1995). The torso receptor tyrosine kinase can activate raf in a ras-independent pathway. *Cell* **81**, 63–71.
- Isaksen, D. E., Liu, N. L., and Weisblat, D. A. (1999). Inductive regulation of cell fusion in leech. *Development* **126**, 3381–3390.
- Jee, W. S. S., and Nolan, P. D. (1963). Origin of osteoclasts from the fusion of phagocytes. *Nature* **200**, 225–226.
- Keely, P. J., Rusyn, E. V., Cox, A. D., and Parise, L. V. (1999). R-Ras signals through specific integrin alpha cytoplasmic domains to promote migration and invasion of breast epithelial cells. *J. Cell Biol.* **145**, 1077–1088.
- Kimberly, E. L., and Hardin, J. (1998). Bottle cells are required for the initiation of primary invagination in the sea urchin embryo. *Dev. Biol.* **204**, 235–250.
- Kimble, J. (1981). Alterations in cell lineage following laser ablation of cells in the somatic gonad of *Caenorhabditis elegans*. *Dev. Biol.* **87**, 286–300.
- Lackner, M. R., Kornfeld, K., Miller, L. M., Horvitz, H. R., and Kim, S. K. (1994). A map kinase homolog, *mpk-1*, is involved in ras-mediated induction of vulval cell fates in *Caenorhabditis elegans*. *Genes Dev.* **8**, 160–173.
- Lane, M. C., Koehl, M. A. R., Wilt, F., and Keller, R. (1993). A role for regulated secretion of apical extracellular matrix during epithelial invagination in the sea urchin. *Development* **117**, 1049–1060.
- Maloof, J. N., and Kenyon, C. (1998). The Hox gene *lin-39* is required during *C. elegans* vulval induction to select the outcome of Ras signaling. *Development* **125**, 181–190.
- Mohler, W. A., Simske, J. S., Williams-Masson, E. M., Hardin, J. D., and White, J. G. (1998). Dynamics and ultrastructure of developmental cell fusions in the *Caenorhabditis elegans* hypodermis. *Curr. Biol.* **8**, 1087–1090.
- Newman, A. P., and Sternberg, P. W. (1996). Coordinated morphogenesis of epithelia during development of the *Caenorhabditis elegans* uterine–vulval connection. *Proc. Natl. Acad. Sci. USA* **93**, 9329–9333.
- Newman, A. P., White, J. G., and Sternberg, P. W. (1996). Morphogenesis of the *C. elegans* hermaphrodite uterus. *Development* **122**, 3617–3626.
- Pierce, G. P., and Midgley, A. R. J. (1963). The origin and function of human syncytiotrophoblastic giant cells. *Am. J. Pathol.* **43**, 153–173.
- Podbilewicz, B. (1996). ADM-1, a protein with metalloprotease- and disintegrin-like domains, is expressed in syncytial organs, sperm and sheath cells of sensory organs in *C. elegans*. *Mol. Biol. Cell* **7**, 1877–1893.
- Podbilewicz, B. (2000). Membrane fusion as a morphogenetic force in nematode development. *Nematology* **2**, 99–111.
- Podbilewicz, B., and White, J. G. (1994). Cell fusions in the developing epithelia of *C. elegans*. *Dev. Biol.* **161**, 408–424.
- Roch, F., Baonza, A., Martin-Blanco, E., and Garcia-Bellido, A. (1998). Genetic interactions and cell behaviour in blistered mutants during proliferation and differentiation of the *Drosophila* wing. *Development* **125**, 1823–1832.
- Schnorr, J. D., and Berg, C. A. (1996). Differential activity of Ras1 during patterning of the *Drosophila* dorsoventral axis. *Genetics* **144**, 1545–1557.
- Schoenwolf, G. C., and Smith, J. L. (1990). Mechanisms of neurulation: Traditional viewpoint and recent advances. *Development* **109**, 243–270.

- Sharma-Kishore, R., White, J. G., Southgate, E., and Podbilewicz, B. (1999). Formation of the vulva in *C. elegans*: A paradigm for organogenesis. *Development* **126**, 691–699.
- Shih, J., and Keller, R. (1994). Gastrulation in *Xenopus laevis*: Involution—a current view. *Dev. Biol.* **5**, 85–90.
- Sternberg, P. W., and Han, M. (1998). Genetics of RAS signaling in *C. elegans*. *Trends Genet.* **14**, 466–472.
- Sternberg, P. W., and Horvitz, H. R. (1989). The combined action of two intercellular signaling pathways specifies three cell fates during vulval induction in *C. elegans*. *Cell* **58**, 679–693.
- Sulston, J. E., and Horvitz, H. R. (1977). Postembryonic cell lineages of the nematode *Caenorhabditis elegans*. *Dev. Biol.* **56**, 110–156.
- Thomas, J. H., and Horvitz, R. H. (1999). The *C. elegans* gene *lin-36* acts cell autonomously in the *lin-35 Rb* pathway. *Development* **126**, 3449–3459.
- Wassarman, D. A., Therrien, M., and Rubin, G. M. (1995). The Ras signaling pathway in *Drosophila*. *Curr. Opin. Genet. Dev.* **5**, 44–50.
- Wu, Y., and Han, M. (1994). Suppression of activated Let-60 Ras protein defines a role of *Caenorhabditis elegans* Sur-1 MAP kinase in vulval differentiation. *Genes Dev.* **8**, 147–159.
- Yanagimachi, R. (1988). Sperm—egg fusion. In “Current Topics in Membranes and Transport” (N. Duzgunes and F. Bonner, Eds.), Vol. 32, pp. 3–43. Academic Press, Orlando, FL.
- Yochem, J., Sundaram, M., and Han, M. (1997). Ras is required for a limited number of cell fates and not for general proliferation in *Caenorhabditis elegans*. *Mol. Cell Biol.* **17**, 2716–2722.
- Zipkin, I. D., Kindt, R. M., and Kenyon, C. J. (1997). Role of a new rho family member in cell migration and axon guidance in *C. elegans*. *Cell* **90**, 883–894.

Received for publication December 2, 1999

Revised February 2, 2000

Accepted February 3, 2000